

# Physicochemical Determination Of CMC And Thermodynamic Evolution: Metallomicelles Of Cr<sup>II</sup>, Mn<sup>II</sup>, And Co<sup>II</sup> Complexes

R. B. Patel<sup>1\*</sup>, N. P. Kapuriya<sup>2</sup>, M. A. Ambasana<sup>3</sup>, J. J. Bhalodia<sup>4</sup>, A. H. Bapodara<sup>5</sup>

<sup>1, 2, 3, 4, 5</sup>Department of Chemistry and Forensic Science, Bhakta Kavi Narsinh Mehta University, Junagadh-362263, Gujarat, India.

\*Email: [rashmipatel@bknmu.edu.in](mailto:rashmipatel@bknmu.edu.in)

DOI: 10.47750/pnr.2022.13.S10.227

## Abstract

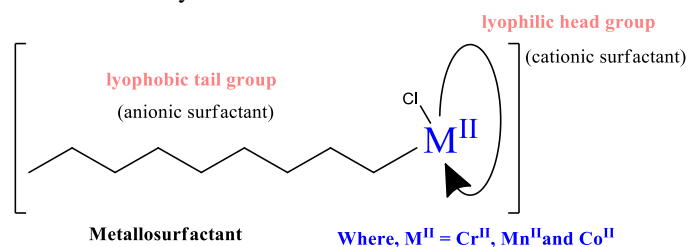
Organometallic surfactants have been synthesised using the heterocyclic ligand 2-((3-methyl -5- oxo -1- phenyl-4,5-dihydro-1H-pyrazol-4-yl)(phenyl)methylene)hydrazine carbothioamide (PMBP-TSC) and transition metal ions (Cr<sup>II</sup>, Mn<sup>II</sup>, and Co<sup>II</sup>). The electrical conductivity at 15, 25, 35 and 45°C, as well as UV-visible spectrophotometry at 25°C, were used to determine the critical micelle concentration (CMC), ionization degree ( $\alpha$ ), degree of counter ion binding ( $\beta$ ), binding constant ( $K_b$ ), and other physicochemical parameters of micellization. These parameters include the standard Gibb's free energy change,  $\Delta_m G^\circ$ , standard enthalpy change,  $\Delta_m H^\circ$ , and standard entropy change,  $\Delta_m S^\circ$ . Based on the negative  $\Delta_m G^\circ$  micellization is thermodynamically possible and spontaneous. The estimate of the activation energy ( $E_a$ ) was estimated using the Coats-Redfern method based on the examination of thermogravimetric analysis (TGA) and the kinetics of thermal degradation. According to the data, adding metal causes the CMC to decrease and the  $E_a$  to rise, proving that Cr<sup>II</sup> has the best level of thermal stability.

**Keywords:** Metallosurfactant, CMC, Physicochemical properties Thermodynamic Micellization, TGA, Activation Energy.

## INTRODUCTION

The novel concept of coordination chemistry is expanding to mumer form, structures, and applications in the mordent chemistry. Numerous physicochemical properties of metallosurfactants including light scattering<sup>1</sup>, electrical conductivity<sup>2</sup>, surface tension<sup>3</sup>, viscosity<sup>4</sup>, self-association into complex structures<sup>5</sup>, aggregation<sup>6</sup>, critical micelle concentration<sup>7, 8</sup>, have been reported to undergo abrupt changes.

The major coordination sphere of the central metal ion in surfactant complexes serves as the lyophilic and lyophobic group of ligands (Scheme 1). There aren't many studies on how such transition M-L surfactant complexes<sup>9</sup> and thermochemistry<sup>10</sup> interact.



The CMC determination indicates to self-aggregation, which causes micelles to form and is thought to be a different process from interfacial adsorption. A reduction in a system's free energy and an increase in entropy, both of which

have a spontaneous process, are symptoms of micelleization<sup>1</sup>. When any of the physicochemical qualities is plotted against the concentration of surfactant molecules, the CMC is defined as the minimal concentration at which surfactant molecules begin to aggregate<sup>11</sup>. Ionic surfactants have a wide range of medicinal activities<sup>12</sup>, including action against bacterial, viral, and fungal infections, leprosy, TB, and leprosy<sup>13, 14, 15</sup>. Their capacity to bind trace metals has frequently been credited as the cause of their action<sup>16</sup>. Thermodynamically different methodological in the determination of the CMC can be found, depending on the used experimental methods<sup>17, 18</sup>. Thermal processing is required to study physical and chemical quantities like mass or enthalpy change, adsorption, crystallization, dehydration, reduction, oxidation, polymerization, chemisorptions, and decomposition are endothermic or exothermic, etc, TGA and DTA is usually used for the kinetic analysis<sup>19, 20</sup> and thermodynamic parameters using many equations including Freeman Carroll, Coats - Redfern, Horowitz - Metzger, Broido, and Piloyan - Novikova of M-L complexes<sup>21</sup>.

In this paper, we discuss the determination of temperature-dependent CMC by the conductometric and UV visible spectrophotometry techniques<sup>22</sup> of Cr<sup>II</sup>, Mn<sup>II</sup>, and Co<sup>II</sup> metal surfactant complexes. The thermal decomposition properties of different coordination surfactants were carried out to assess their  $E_a$  and pre exponential factor (A) by Coats-Redfern method<sup>23</sup>.

## EXPERIMENTAL

### Materials and Solutions

Analytical grade hexahydrate chloride salts of Cr<sup>II</sup>, Mn<sup>II</sup>, and Co<sup>II</sup>, gradient grade MeOH from Sigma Aldrich with the highest purity of > 99.5 %. The conductivity of the solvent was  $< 3.0 \times 10^{-7} \text{ Scm}^{-1}$  at 25°C temperature. All reagents Benzoyl chloride, Calcium hydroxide, Ethyl acetoacetate, Phenyl hydrazine, 1, 4 Dioxane and Glacial acetic acid were purchased from finar chem. Ltd., Ahmadabad, Gujarat.

A digital conductometer used to measure the electronic conductance (Metrohm- 856). The conductivity cell was calibrated with KCl (Marck) in deionized water in the appropriate concentration (0.001, 0.01, 0.1 mol dm<sup>-1</sup>). A water-bath type thermostat and a cell made of pt-black with a cell constant of 0.99 cm<sup>-1</sup> were used to maintain the solution's temperature with an accuracy of  $\pm 0.2^\circ\text{C}$ .

Using a UV-visible spectrophotometer model JASCO V-530 with a cuvette (quartz) 1.0 cm path length, the electronic absorption spectra of the various metallosurfactants were conducted in the range of 200-800 nm. At a scan speed of 400 nm min<sup>-1</sup>, all spectra were captured. The materials were weighed using an analytical balance with a readability of 0.0001 g made by Sartorius (Bradford, MA, USA).

### Synthesis and Characterization of Metallosurfactant

The surfactant complexes of ligand PMBP-TSC and their Cr<sup>II</sup>, Mn<sup>II</sup>, and Co<sup>II</sup> were syntheses by green method, and characterization was briefly described in our previous publication<sup>24</sup>.

## PHYSICO-CHEMICAL METHODS

### Electric Conductance Measurement

In a typical experiment, 50 ml of the metal salt solution ( $2.0 \times 10^{-4} \text{ M}$ ) in methanol was placed in the titration cell. The thermostated circulator water bath was joined to maintain a constant temperature and the observed conductance of the solution was measured. Then a 0.2 mL of ligand ( $2.0 \times 10^{-3} \text{ M}$ ) in methanol was added in a stepwise manner using a calibrated micro burette and the conductance of the solution was measured after the string of each addition (1.0 min) and thermal equilibration. A similar method was followed at the temperature range from 15 to 45°C and the conductometry data were used for the calculation of the CMC of the complexes in organic polar solvent methanol at the preferred temperatures.

### UV – Visible Absorption Spectrophotometric Method

0.2 ml of the PMBP-TSC ( $2.0 \times 10^{-3}$  M) solution in methanol was placed in the UV- visible spectrophotometer unit and measured its absorbance. Then a series of fixed  $2.0 \times 10^{-4}$  M of metal ions were added stepwise by using a 10 ml micropipette and after each addition of the solution, the absorbance was recorded at the respective wavelength maximum ( $\lambda_{\text{max}}$ ). The CMC was achieved at 25°C temperature. The value of the reported rate constant was given as an average of duplicate runs.

## THERMODYNAMICS OF MICELLIZATION

### Critical Micelle Concentration Critical and Degree of Micelle Ionization

The standard technique of calculating the CMC used electrical conductivity. The experimental curve's breakpoint was identified by plots of specific conductance ( $\kappa$ ) vs. surfactant concentration (c) and absorbance versus surfactant concentrations<sup>25</sup>. The slope ratio at the pre-post micellar regions point of the curve can be used to estimate the degree of micelle ionisation ( $\beta$ ). The first rising portion of the picture with slope  $P_1$  is caused by the conductivity of free surfactant ions,  $\lambda_+$ , and their corresponding counter ions,  $\lambda_-$ , rising owing to an increase in surfactant concentration,  $C_s$ , in solution.

$$\kappa = (\lambda_+ + \lambda_-)C_s = P_1.C_s \quad (1)$$

According to the mass-action model, it is predicted that the concentration of surfactant ions above the critical micelle concentration stays close to the CMC, only causing the concentration of the micelle and its corresponding counter ion to increase with surfactant addition.

$$\kappa = (\lambda_+ + \lambda_-)cmc + \frac{C_s - cmc}{n}\lambda_m + (C_s - cmc)\beta.\lambda_- \quad (2)$$

A post micellar slope of specific conductivity versus surfactant concentration plot,  $P_2$ , can be thus expressed as,

$$\frac{\kappa - (\lambda_+ + \lambda_-)cmc}{C_s - cmc} = \frac{1}{n}\lambda_m + \beta.\lambda_- = P_2 \quad (3)$$

Its ionic molar conductivity,  $\lambda_m$  assumed to be proportional to the molar conductivity of free surfactant ion, taking an effectual charge of the micelle,

$$\lambda_m = z.\lambda_+ \quad (4)$$

( $\therefore z = n.\beta$ ,  $n =$  micelle aggregation number), as the proportionality constant.

$$\lambda_m = n.\beta.\lambda_+ \quad (5)$$

From Eq. (1), (3), and (4),  $\beta$  can be calculated as the ratio among the minimum and the maximum slope of the specific conductivity against surfactant concentration below and above the CMC<sup>7</sup>.

$$\beta = \frac{P_2}{P_1} \quad (6)$$

Thermodynamic  $\Delta_m G^\circ$  for ionic surfactants was determined by using the following equation<sup>26</sup>.

$$\Delta_m G^\circ = (2 - \beta) RT \ln X_{\text{CMC}} \quad (7)$$

Where,  $\beta$  is the counter ion dissociation constant,  $R$  ( $8.314 \text{ J K}^{-1} \text{ mol}^{-1}$ ) is the gas constant,  $T$ , the temperature in Kelvin and  $X_{\text{CMC}}$  stands for the CMC in the mole fraction unit. For nonionic surfactant solution with or without co- solute  $\Delta_m G^\circ$  was obtained by the following relation:

$$\Delta_m G^\circ = RT \ln X_{\text{CMC}} \quad (8)$$

The  $\Delta_m S^\circ$  was calculated from the temperature dependence of  $\Delta_m G^\circ$  using the relation,

$$\Delta_m S^\circ = - \frac{d\Delta_m G^\circ}{dT} \quad (9)$$

The micelle formation of  $\Delta H_m^\circ$  was derived from Gibb's Helmholtz equation:

$$\Delta_m H^\circ = \Delta_m G^\circ + T\Delta_m S^\circ \quad (10)$$

## THERMOGRAVIMETRIC ANALYSIS (TGA)

The TGA analyses with detector DTG-60H were carried out on nitrogen atmosphere at 50°C to 800°C with a flow rate of 100 ml per minute and an alumina cell. The weight of the samples was ~5-7 mg taken to an evaluation of the  $E_a$ , which was calculated by the method of A.W. Coats and J. P. Redfern<sup>27</sup> based on the hypothesis that the single

stage 1<sup>st</sup> order reactions, it was submitted to the Arrhenius laws occur, are progress. The data were obtained using a weight loss versus temperature plot.

### Kinetic Treatment

A mathematical model developed by Coats and Redfern was used for kinetic analysis of the data generated by the TGA experiment. Solid-phase thermal decomposition is described by the rate of expression by following equation:

$$\frac{d\alpha}{dt} = k(1 - \alpha)^n \quad (11)$$

Where k is a rate constant, t is reaction time; n is the order of reaction, Conversion  $\alpha$  at a time t is defined by,

$$\alpha = \frac{(\omega_i - \omega_t)}{(\omega_i - \omega_\infty)} \quad (12)$$

Where  $\omega_i$  and  $\omega_\infty$  are initial and final sample weight (mg) and  $\omega_t$  (mg) is the weight at a time t. In general, the Arrhenius equation may be used to explain how the reaction rate constant varies with temperature. The response rate for a solid's breakdown may be defined as,

$$k = A \cdot e^{E_a/RT} \quad (13)$$

Where, A = pre-exponential factor ( $\text{min}^{-1}$ ),  $E_a$  = activation energy ( $\text{kJ mole}^{-1}$ ). For a linear heating rate,  $\beta$  in degrees Celsius per minute,

$$\beta = \frac{dT}{dt} \quad (14)$$

By combining Eq. 11 and 14, rearranging, integrating, and taking the natural logarithm,

$$\ln \left[ \frac{1 - (1 - \alpha)^{1-n}}{T^2(1 - n)} \right] = \ln \frac{F_p R}{\beta E_a} \left( 1 - \frac{2RT}{E_a} \right) - \left( \frac{E_a}{R} \right) \frac{1}{T} \quad (15)$$

For all values of n except when n = 1.

$$\ln \left[ \frac{-\ln(1 - \alpha)}{T^2} \right] = \ln \frac{F_p R}{\beta E_a} \left( 1 - \frac{2RT}{E_a} \right) - \left( \frac{E_a}{R} \right) \frac{1}{T} \quad (16)$$

Therefore, a plot of  $\ln[1 - (1 - \alpha)^{1-n}/T^2(1 - n)]$  against  $1/T$  or for  $n=1$ ,  $\ln[-\ln(1 - \alpha)/T^2]$  against  $1/T$  should yield a straight line with a slope ( $E_a/R$ ) for the correct value of n.

## RESULTS AND DISCUSSION

Chemical structures and characterization of the various transition metal-based surfactants were described in detail in our previous work<sup>24</sup>. Physico-chemical detail of the ligand and their M-complexes are shown in Table 1. The electrical conductometric study of surfactant  $\text{Cr}^{\text{II}}$ ,  $\text{Mn}^{\text{II}}$ , and  $\text{Co}^{\text{II}}$  complexes with PMBP-TSC was done by conductometry and UV-visible spectrophotometry. The CMC value can be determined graphically according to Williams<sup>28</sup>. The result shows that the slope of the resultant lines corresponds to the estimate  $\beta$  evolves by the help of Eq. (16). Typical plots are given in Fig. 1 (a, b, and c). All results are summarized in Table 2. Show one evident graph, suggestive that the probability stoichiometric ratio of metallosurfactants is M: L and the Micelle formation concentration as a function of the molar concentrations against temperature.

Table-1: Physical data of the Ligand and their Metal-Complexes

Compounds	M. Wt.	M.P./ °C	Colour	$\Lambda_{\text{m}\mu\text{S}}$	$\lambda_{\text{max}}$
$\text{L}(\text{C}_{18}\text{H}_{17}\text{N}_5\text{OS})$	351.43	203	White	-	
$\text{C}_{18}\text{H}_{16}\text{ClCrN}_5\text{OS}$	437.87	220	Dark green	85.6	238
$\text{C}_{18}\text{H}_{16}\text{ClMnN}_5\text{OS}$	440.81	215	Brown	79.7	246
$\text{C}_{18}\text{H}_{16}\text{ClCoN}_5\text{OS}$	444.80	281	Grey	72.3	250

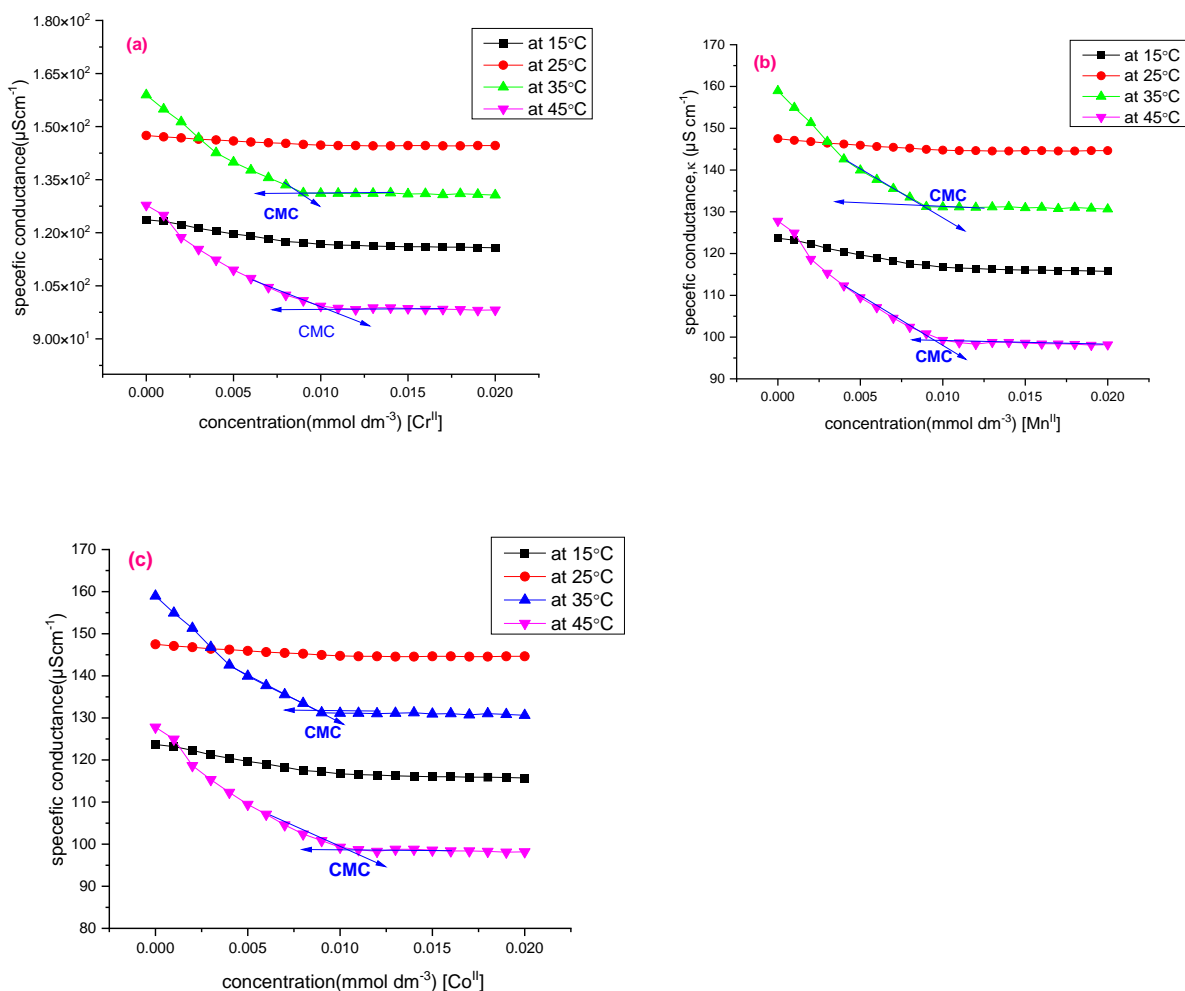


Fig.1. Plot of variation  $\kappa$  against  $[c]$  of (a)  $\text{Cr}^{\text{II}}$ , (b)  $\text{Mn}^{\text{II}}$  and (c)  $\text{Co}^{\text{II}}$  complexes in methanol at different temperature.

Table-2: Ionization degree ( $\alpha$ ) and Degree of Counter ion Binding ( $\beta$ ) by Conductivity

Complexes	Temp. (K)	Specific Conductance ( $\kappa$ )	CMC $\times 10^{-4}$	$\alpha$	$\beta$
[Cr(PMBP-TSC) . 3H <sub>2</sub> O]	288	131.026	0.0101	0.105391	0.894609
	298	171.206	0.01	0.021256	0.978744
	308	167.7819	0.00994	0.018787	0.981213
	318	105.056	0.00981	0.083381	0.916619
[Mn(PMBP-TSC) .H <sub>2</sub> O]	288	135.338	0.01025	0.053748	0.946252
	298	159.446	0.01013	0.21709	0.78291
	308	156.604	0.01004	0.079768	0.920232
	318	144.158	0.00993	0.121666	0.878334
[Co(PMBP-TSC) . 3H <sub>2</sub> O]	288	116.72	0.01015	0.109753	0.890247
	298	144.746	0.01001	0.012154	0.987846
	308	131.124	0.00995	0.014289	0.985711

The calculated thermodynamic parameters of  $\Delta_m H^\circ$ ,  $\Delta_m S^\circ$ , and  $\Delta_m G^\circ$  are listed in Table 3. In the micellar aggregation numbers<sup>29</sup>, we observed that the order of aggregation number is  $Mn^{II} > Cr^{II} > Co^{II}$ . The effect of temperature on the CMC of surfactant in pure methanol, Fig. 2, shows the Micelle formation concentration as a function of the molar concentrations against temperature, it is evident that the CMC decreases with increasing temperature. In Fig. 3, we represent the temperature dependent of the degree of ionization ( $\alpha$ ), of the metalosurfactant in methanol.

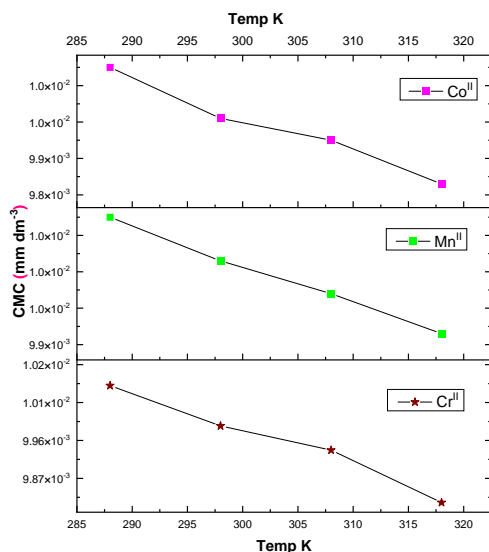


Fig.2. The Plots of CMC of micelle formation of metalosurfactants in methanol at different temperature.

Table -3: Thermodynamic Parameters of Metalosurfactant at Different Temperature

Surfactants	Temp. (K)	CMC (mol dm <sup>-1</sup> )	Thermodynamic parameters			
			$\Delta G_k Jmol^{-1}$	$\Delta H kJmol^{-1}$	$\Delta S Jmol^{-1}$	log K <sub>b</sub>
Cr <sup>II</sup>	288	0.0101	-20.8463	1.30E+00	4.586361	21.67389
	298	0.0100	-22.5768	1.17E+00	3.99	24.288123
	308	0.00994	-23.394	1.50E+00	4.941979	26.011863
	318	0.00981	-23.4328	2.13E+00	6.762467	26.900919
Mn <sup>II</sup>	288	0.01025	-21.3458	1.58E+00	5.573116	22.216944
	298	0.01013	-20.2853	1.37E+00	4.662052	22.193854
	308	0.01004	-22.6247	1.51E+00	4.976074	25.156509
	318	0.00993	-22.9043	1.74E+00	5.534666	26.294248
Co <sup>II</sup>	288	0.01015	-20.7759	1.81E+00	6.363373	21.600757
	298	0.01001	-22.6757	1.46E+00	4.976785	24.39455
	308	0.00995	-23.442	1.42E+00	4.689494	26.065238
	318	0.00983	-24.1784	2.01E+00	6.405292	27.756866

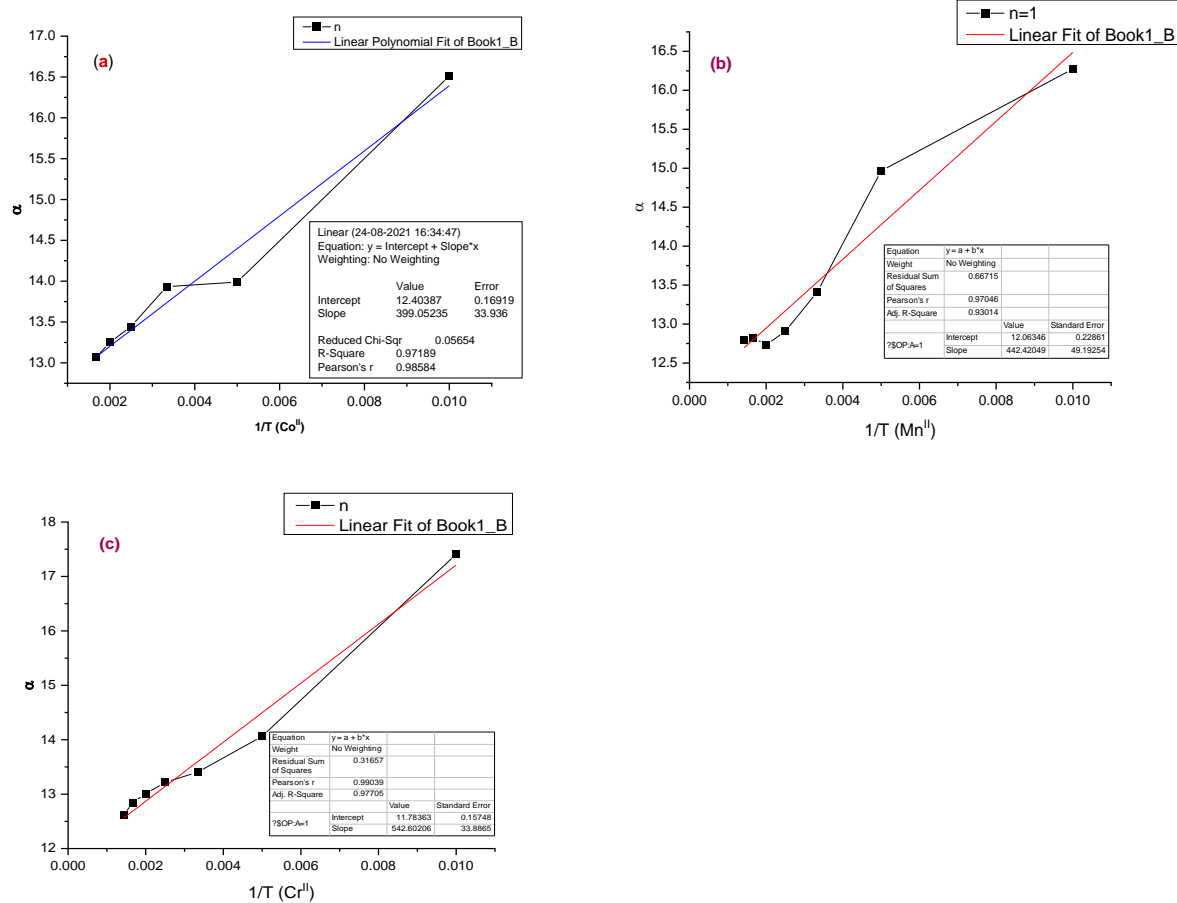


Fig. 3. The plot of  $\alpha$  vs.  $1/T$  (K) of (a) Cr<sup>II</sup>, (b) Mn<sup>II</sup> and (c) Co<sup>II</sup> metallosurfactants in methanol.

Figure 4 (a, b, and c) shows the  $\Delta_m G^\circ$ ,  $\Delta_m H^\circ$ , and  $\Delta_m S^\circ$  of metallosurfactant and temperature exhibit a linear relation. This phenomenon is called  $\Delta_m H^\circ - \Delta_m S^\circ$  compensation<sup>30</sup>. The  $\Delta_m G^\circ$  decreases with rising temperature. The negative value for the observed systems of micellization process, which indicates the feasibility of the micelle formation, is favored thermodynamically. The binding constant  $K_b$  is derived by the following relationship,

$$\Delta_m G^\circ = -2.303RT \log K_b \quad (17)$$

The values of  $\Delta H_m^\circ$  and  $\Delta S_m^\circ$  were positive and decreased with the temperature range [15 to 45 °C] indicating that the micellization process becomes endothermic.

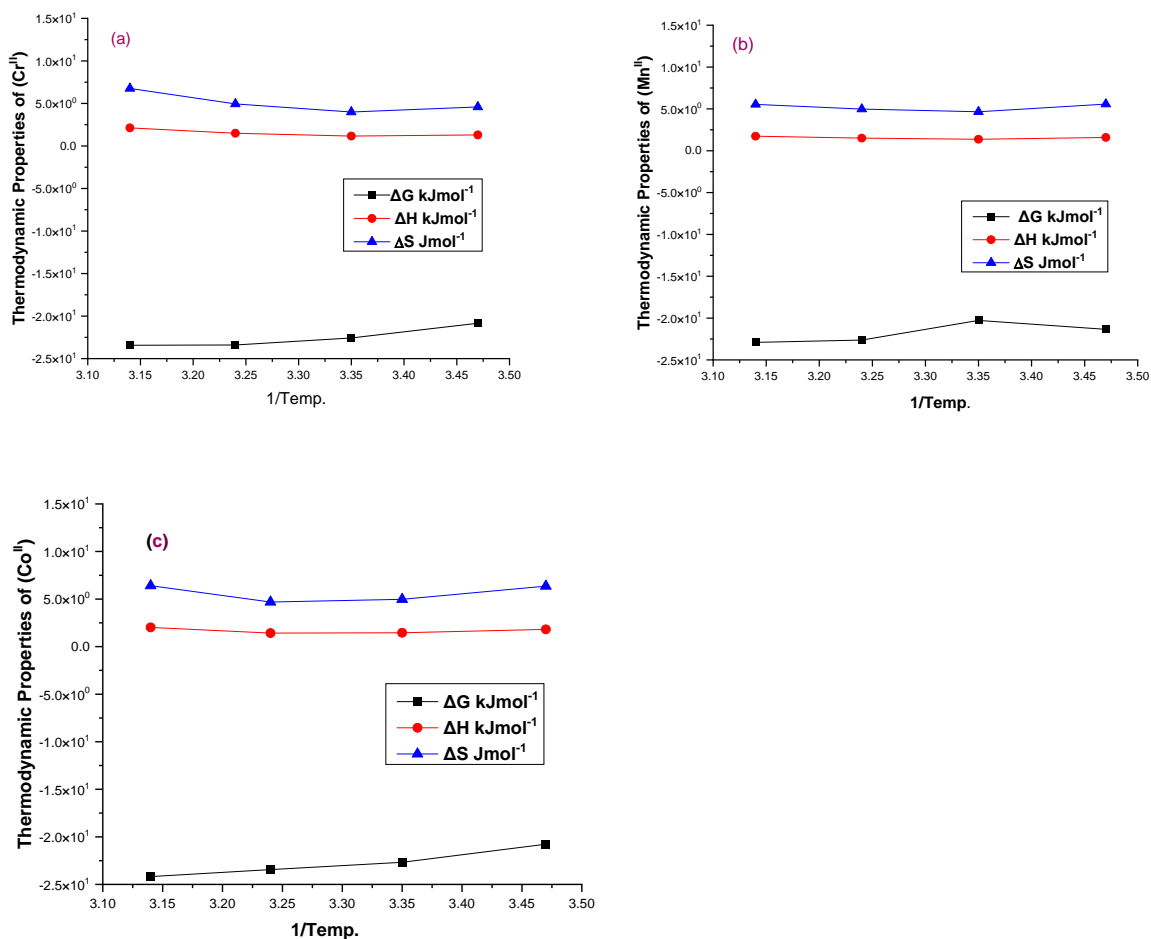


Fig.4. Plots of Thermodynamic properties  $\Delta_m G^\circ$ ,  $\Delta_m H^\circ$  and  $\Delta_m S^\circ$  of Cr<sup>II</sup>, Mn<sup>II</sup> and Co<sup>II</sup>, metallosurfactants in methanol at different temperature.

The UV-visible spectrum of M: L surfactant shows the variation effect of absorbance with the wavelength in Fig. 5 (a, b and c). The CMC determine by the plot of absorbance against concentrations of various metallosurfactant at 25°C temperature Fig. 6.



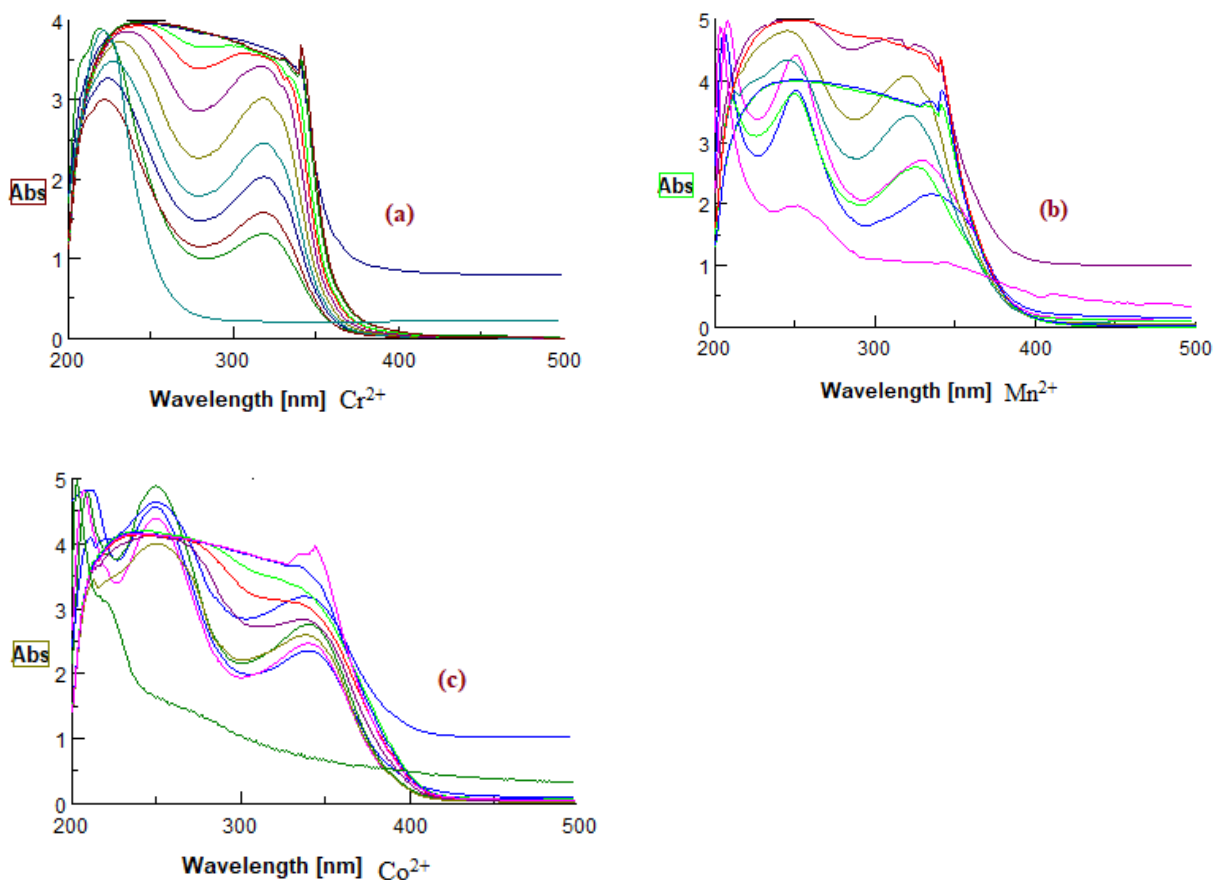


Fig. 5. The Plots of UV- visible spectrum of metallosurfactants (a) Cr<sup>II</sup>, (b) Mn<sup>II</sup> and (c) Co<sup>II</sup> in methanol at 25 °C temperature.

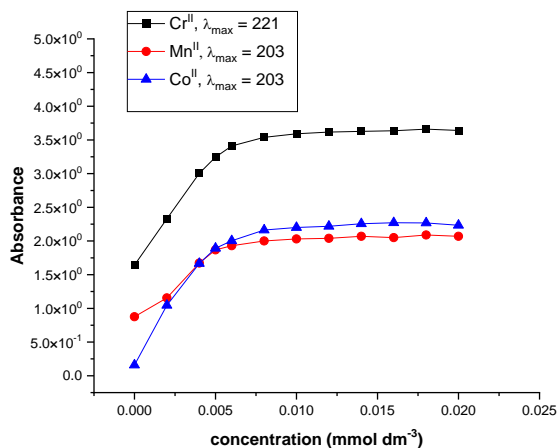


Fig. 6. The Plots of Absorbance vs. concentration metallosurfactants of Cr<sup>II</sup>, Mn<sup>II</sup> and Co<sup>II</sup> in methanol at 25 °C temperature.

The TGA graph of the metallosurfactant Cr<sup>II</sup> (C<sub>3</sub>), Mn<sup>II</sup> (C<sub>5</sub>), and Co<sup>II</sup> (C<sub>6</sub>) complex (Fig. 7), the 1<sup>st</sup> stage of weight loss ranged from 50°C to around 200°C was distinct from the other stages. It corresponds to the loss of coordinated water part and the loss of ligand parts. In the 1<sup>st</sup>, there was mass (< 0.87%) in the range of 50–100°C and > 5.04% in

the range of 100–200°C. The 2<sup>nd</sup> phase of weight loss started ~250°C. The plot of the region between 250 and 800°C exploded was mass loss >77.27%. The value of E<sub>a</sub> obtained graphically is substituted in Eq. (15 or 16) to calculate the pre-exponential factor, F<sub>p</sub>. Eq. (13) is used to estimate the rate constant at any temperature is presented in Table 4.

Table-4: Thermal data and lnCMC value of Metallosurfactant at 25°C temperature

Surfactants	Electric Conductometry	UV-Visible Absorbance Spectroscopic	TGA Analysis (E <sub>a</sub> )
[Cr(L).3H <sub>2</sub> O]	-4.6052	-4.62957	4512.839
[Mn(L).H <sub>2</sub> O]H <sub>2</sub> O	-4.5923	-4.56595	3674.788
[Co(L).3H <sub>2</sub> O]	-4.5952	-4.62957	3317.28

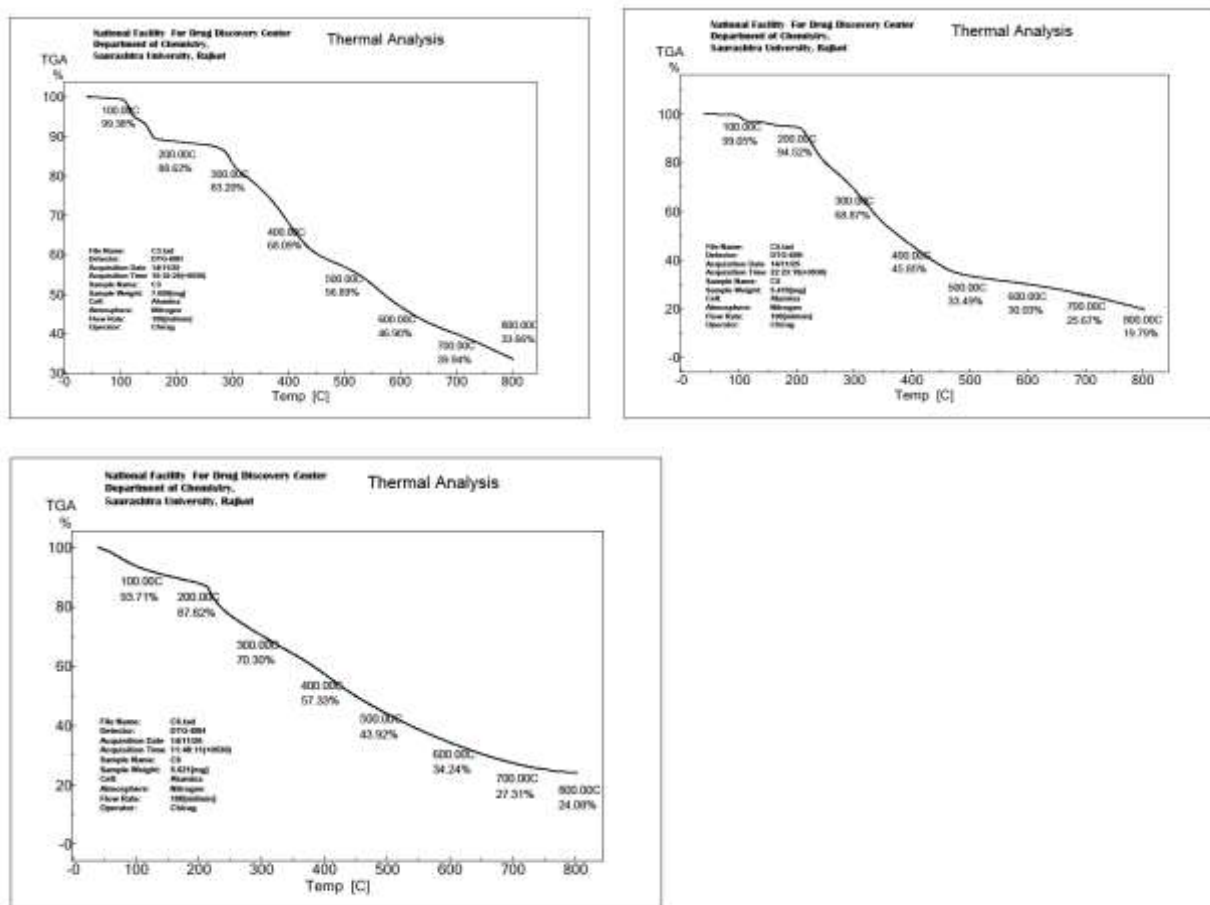


Fig. 7. TGA graph of (C<sub>6</sub>) Cr<sup>II</sup>, (C<sub>5</sub>) Mn<sup>II</sup> and (C<sub>3</sub>) Co<sup>II</sup> metallosurfactants.

## CONCLUSION

The physic-chemical parameters of metallosurfactant were studied using conductometry and UV-visible spectrophotometer. From the result obtained, the specific conductivities and value of CMC are found to decrease with the increased temperature and concentration of transition metal surfactant in the presence of methanol. The negative value of Δ<sub>m</sub>G° indicated the spontaneity and the positive value of Δ<sub>m</sub>H° being endothermic nature and positive Δ<sub>m</sub>S° showed the endothermic nature.

According to TGA findings, thermal degradation of metallosurfactants occurs in two phases, with the 1<sup>st</sup> stage beginning at 50°C and ending at 200°C, and the 2<sup>nd</sup> stage occurring between 220°C and 600°C. The results concluded that estimated Ea decreasing order Cr<sup>II</sup> > Mn<sup>II</sup> > Co<sup>II</sup>.

## ACKNOWLEDGMENT

The Department of Chemistry and Forensic Science at Bhakta Kavi Narsinh Mehta University in Junagadh provided the writers with the required facilities, while UGC-Info Net and INFLIBNET Gujarat University provided e-source services.

## REFERENCES

- [1] K.M. Sachin, S.A. Karpe, M. Singh, A. R. Bhattarai, Soc. Open Sci., **6**, 181979(2019). DOI: <http://dx.doi.org/10.1098/rsos.181979>.
- [2] H. Demissie, R. Duraisamy, J. Sci. Innov. Res., **5**, 208-214(2016).
- [3] N. Rehman, H. Ullah, S. Alam, A. Khaliq Jan, S. W. Khan, M. Tariq, J. Mater. Environ. Sci. **8**, 1161-1167(2017).
- [4] Z. Haq, N. Rehman, F. Ali, N. Mehmood Khan H. Ullah, J. Mater. Environ. Sci., **8**, 1029-1038(2017).
- [5] M.M. Alejandro, C.R. Juan, R.A. Lena, C.N. Ernesto, Chem. Cent. J., **10**, (2016). DOI: 10.1186/s13065-016-0213-9.
- [6] S. Muhammad, K. Muhammad, S. Muhammad, J. Chem. Sci., **127**, 2073–2079(2015). DOI: 10.1007/s12039-015-0975-y.
- [7] A. Kroflic, B. Sarac, M. Bester-Rogac, Acta. Chim. Slov., **59**, 564–570(2012).
- [8] J. Oremusov, Z. Vitkov, A. Vitko, M. Tamik,, E. Miklovicova, O. Ivankova, J. Murgas, Molecules, **24**, 651(2019). DOI: 10.3390/molecules24030651.
- [9] J.R.B. Gomes, M.A.V. Ribeiro da Silva, Curr. Phys. Chem., **1**, 55-64 (2011).
- [10] R.K. Ameta, M. Singh, Heliyon, **5**, (2019). DOI: 10.1016/j.heliyon.2019.
- [11] N. Azum, D. Kumar, Sci. Rep., **10**, 4088(2020). DOI: <https://doi.org/10.1038/s41598-020-61001-6>
- [12] N.A. Negm, D.E. Mohamed, M.M. Said, A. Abdel Aal, J. Appl. Chem. (IOSR-JAC), **7**, 86-96(2014).
- [13] G. Vignesh, K. Sugumar, S. Arunachalam, S. Vignesh, J.R. Arthur, R. Arunc, K. Premkumarc, Luminescence (2015). DOI: 10.1002/bio.2991.
- [14] M.F. Zaky, A.M. Badawi, I.A. Sabbah, R.A. Abd Elghani, E.A. Ismaeil, M.E. Hendawy, Egypt. J. Chem., **55**, 259-275(2012).
- [15] K. Akhter, K. Ullah, R. Talat, A. Haider, N. Khalid, F. Ullah, S. Ali, Heliyon, **5**(2019). DOI: <https://doi.org/10.1016/j.heliyon.2019.e01885>.
- [16] G.A. Soomro, G.A. Shar, J. Chem. Org., **10**, 95-104(2014).
- [17] M. Prasad, R. Palepu, S.P. Moulik, Colloid Polym. Sci., **284**, 871-878(2006). DOI: 10.1007/s00396-005-1453-8.
- [18] K.S. Sharma, S. R. Patil, A.K. Rakshit, J. Phys. Chem. B, **108**, 12804-12812(2004).
- [19] X. Wang, W. Sizhu, K. Wang, Curr. Phys. Chem., **1**, 65-68(2011).
- [20] C.R.L. Fernanda, K. Tannous, J. Yesid, O. Rueda, Bioresour. Technol., **219**, 392–402(2016). DOI: <http://dx.doi.org/10.1016/j.biortech.2016.07.099>.
- [21] A. Joram, R. Sharma, A.K. Sharma, Open Chem. J., **5**, 145-157(2018). DOI: 10.2174/1874842201805010145.
- [22] B.A.A. Najri, Ph.D. Thesis, The Al-Azhar University-Gaza Deanship of Postgraduate Studies Faculty of Science, Department of Chemistry, June (2016).
- [23] A.W. Coats, J.P. Redfern, Kinetic. Nature, **201**, 68-69(1964).
- [24] R.B. Patel, D.P. Rajani, S.D. Rajani, H.D. Patel, J. Phy. Chem. Sci., **3**, 2348 – 327X (2015).
- [25] O. Chidi, I.V. Adebayo, Mod. Chem. Appl., **6**, 251(2018). DOI: 10.4172/2329-6798.1000251
- [26] J.J. Gala, A. Gonza lez-Perez, J.A. Seijas, E. Uriarte, J.R. Rodriguez, Colloid Polym. Sci., **283**, 456–46(2005). DOI: 10.1007/s00396-004-1206-0.
- [27] A. Dariga, A. Alexander, T., Roman, MATEC Web of Conferences, **194**(2018). DOI: <https://doi.org/10.1051/mateconf/201819401058>.
- [28] J.Y. Hisham, J. El-Aila. Dispers. Sci. Techno., **31**, 557–562(2010). DOI: 10.1080/01932690903192549.
- [29] A. Mudawadkar, T. Patil, J. Chem. Sci. Trans., **5**, 149-162(2016).
- [30] L. Tennouga, A. Mansri, K. Medjahed, A. Chetouani, I. Warad, J. Mater. Environ. Sci., **6**, 2711-2716(2015).